REPORT DOCUMENTATION PAGE

Form Approved OMB NO. 0704-0188

1. REPORT DATE (DD-MM-YYYY)	2. REPORT TYPE	3. DATES COVERED (From - To)
24-06-2013	Final Report	26-Sep-2012 - 31-Mar-2013

4. TITLE AND SUBTITLE
FINAL REPORT

5a. CONTRACT NUMBER

5b. GRANT NUMBER
W911NF-12-C-0102

5c. PROGRAM ELEMENT NUMBER
665502

665502

6. AUTHORS
Hongjun Zeng, Michael McAlpine

5d. PROJECT NUMBER

5e. TASK NUMBER

5f. WORK UNIT NUMBER

7. PERFORMING ORGANIZATION NAMES AND ADDRESSES
Advanced Diamond Technologies, Inc.
48 E. Belmont Drive

Romeoville, IL 60446 -1764

8. PERFORMING ORGANIZATION REPORT NUMBER

9. SPONSORING/MONITORING AGENCY NAME(S) AND ADDRESS(ES)
U.S. Army Research Office
P.O. Box 12211
Research Triangle Park, NC 27709-2211

10. SPONSOR/MONITOR'S ACRONYM(S)
ARO

11. SPONSOR/MONITOR'S REPORT NUMBER(S)
62530-EG-ST1.1

12. DISTRIBUTION AVAILIBILITY STATEMENT
Approved for Public Release; Distribution Unlimited

13. SUPPLEMENTARY NOTES
The views, opinions and/or findings contained in this report are those of the author(s) and should not contrued as an official Department of the Army position, policy or decision, unless so designated by other documentation.

14. ABSTRACT
In this month, the team mostly focused on diamond deposition. Diamond films with 4 boron doping levels were deposited. Although this month's work revealed some challenges in accurately controlling the resistivity in the diamond films, the films were manufactured successfully and will be delivered on time. Part of the characterization of the diamond films including thickness, resistivity, residual stress and Raman spectra measurement is finished. Raman spectra shows basically regular nanocrystalline diamond signature as expected.(continued in report)

15. SUBJECT TERMS
strain-modulated, synthesized diamond film, nanoribbons, electron/hole mobility, flexoelectricity, piezoresistivity, biocompatibility,

16. SECURITY CLASSIFICATION OF:			17. LIMITATION OF ABSTRACT	15. NUMBER OF PAGES	19a. NAME OF RESPONSIBLE PERSON
a. REPORT	b. ABSTRACT	c. THIS PAGE			Hongjun Zeng
UU	UU	UU	UU		19b. TELEPHONE NUMBER 815-293-0900

Report Title

FINAL REPORT

ABSTRACT

In this month, the team mostly focused on diamond deposition. Diamond films with 4 boron doping levels were deposited. Although this month's work revealed some challenges in accurately controlling the resistivity in the diamond films, the films were manufactured successfully and will be delivered on time. Part of the characterization of the diamond films including thickness, resistivity, residual stress and Raman spectra measurement is finished. Raman spectra shows basically regular nanocrystalline diamond signature as expected. (continued in report)

Enter List of papers submitted or published that acknowledge ARO support from the start of the project to the date of this printing. List the papers, including journal references, in the following categories:

(a) Papers published in peer-reviewed journals (N/A for none)

Received Paper

TOTAL:

Number of Papers published in peer-reviewed journals:

(b) Papers published in non-peer-reviewed journals (N/A for none)

Received Paper

TOTAL:

Number of Papers published in non peer-reviewed journals:

(c) Presentations

Number of Presentations: 0.00

Non Peer-Reviewed Conference Proceeding publications (other than abstracts):

Received Paper

TOTAL:

Number of Non Peer-Reviewed Conference Proceeding publications (other than abstracts):

Peer-Reviewed Conference Proceeding publications (other than abstracts):

Received Paper

TOTAL:

Number of Peer-Reviewed Conference Proceeding publications (other than abstracts):

(d) Manuscripts

Received Paper

TOTAL:

Number of Manuscripts:

Books

Received Paper

TOTAL:

Patents Submitted

Patents Awarded

Awards

Graduate Students

NAME	PERCENT_SUPPORTED	Discipline
Yong Lin Kong	0.10	
FTE Equivalent:	**0.10**	
Total Number:	**1**	

Names of Post Doctorates

NAME	PERCENT_SUPPORTED
FTE Equivalent:	
Total Number:	

Names of Faculty Supported

NAME	PERCENT_SUPPORTED	National Academy Member
Michael McAlpine	0.00	
FTE Equivalent:	**0.00**	
Total Number:	**1**	

Names of Under Graduate students supported

NAME	PERCENT_SUPPORTED
FTE Equivalent:	
Total Number:	

Student Metrics

This section only applies to graduating undergraduates supported by this agreement in this reporting period

The number of undergraduates funded by this agreement who graduated during this period:	0.00
The number of undergraduates funded by this agreement who graduated during this period with a degree in science, mathematics, engineering, or technology fields:.....	0.00
The number of undergraduates funded by your agreement who graduated during this period and will continue to pursue a graduate or Ph.D. degree in science, mathematics, engineering, or technology fields:.....	0.00
Number of graduating undergraduates who achieved a 3.5 GPA to 4.0 (4.0 max scale):	0.00
Number of graduating undergraduates funded by a DoD funded Center of Excellence grant for Education, Research and Engineering:	0.00
The number of undergraduates funded by your agreement who graduated during this period and intend to work for the Department of Defense	0.00
The number of undergraduates funded by your agreement who graduated during this period and will receive scholarships or fellowships for further studies in science, mathematics, engineering or technology fields:	0.00

Names of Personnel receiving masters degrees

NAME
Total Number:

Names of personnel receiving PHDs

NAME
Total Number:

Names of other research staff

NAME	PERCENT_SUPPORTED
Prabhu Arumubam	0.10
John Carlisle	0.10
Hongjun Zeng	0.10
FTE Equivalent:	**0.30**
Total Number:	**3**

Sub Contractors (DD882)

1 a. Princeton University

1 b. Office of Research & Project Administra
PO Box 36
Princeton NJ 08544

Sub Contractor Numbers (c): W911-12-C-0102-1
Patent Clause Number (d-1): FAR 52.227-2
Patent Date (d-2):
Work Description (e): Assist in development of CVD diamond film; perform testing
Sub Contract Award Date (f-1): 9/26/2012 12:00:00AM
Sub Contract Est Completion Date(f-2): 3/25/2013 12:00:00AM

Inventions (DD882)

Scientific Progress

<Included in attached report>

Technology Transfer

REPORT DOCUMENTATION PAGE (SF298)
(Continuation Sheet)

Final Project Report 09/27/12 – 03/25/13

Abstract

In this STTR phase I project, Advanced Diamond Technologies worked with Princeton University to fabricate and characterize Strain-Modulated Diamond Nanostructures for Next-Generation, Biocompatible Nanoelectromechanical Systems. During the 6-month work effort, all three major tasks including the subtasks are accomplished on time. We have accomplished the following: 1) Delivered diamond film with designed thinness, grain size and doping levels for the fabrication of diamond nanoribbons. 2) Developed stress control of diamond film to facilitate ribbons release; 3) Studied pinhole density of diamond film and developed two new methods to decrease pinhole density for super thin (<100 nm) film; 4) fabricated diamond nanoribbons with diamond films of different doping levels and thicknesses. Notably, a 50-nm-thick film was demonstrated with good electrical continuity. 5) Characterized diamond nanoribbons with SEM, EDS, AFM, Resistivity and gate effect measurement. Methods to improve the gate effect of diamond film were proposed. ; 6) Established Fluorescence fibrinogen test protocol, which was accomplished mostly by systematic fibrinogen test on different diamond surfaces. 7) Optimized EG6 diamond surface functionalization protocol and demonstrated the capability of bio-interfaced diamond nanoribbons for selective biosensing applications. Based on these results achieved during the Phase I project, we are encouraged and ready to advance in the phase II portion of the project.

TECHNICAL REPORT COVER INFORMATION	
1a. CONTRACT NUMBER W911NF-12-C-0102	1b. PROPOSAL NUMBER A12A-017-0282
2. CONTRACTOR NAME AND ADDRESS Advanced Diamond Technologies, Inc. 48 E. Belmont Drive Romeoville, IL 60446	
3. PROJECT TITLE Strain-Modulated Diamond Nanostructures for Next-Generation, Biocompatible Nanoelectromechanical Systems	
4. CONTRACT PERFORMANCE PERIOD 09/27/2012 - 03/25/2012	PERIOD OF THIS REPORT 02/26/2013 - 03/25/2013
5. TOTAL CONTRACT AMOUNT $99,667	8. NUMBER OF EMPLOYEES ON THE PROJECT THIS MONTH 8
6.FUNDS PAIDS BY DFAS TO DATE $83,056	9. NUMBER OF NEW EMPLOYEES PLACED ON CONTRACT THIS MONTH 0
7. TOTAL EXPENDED/INVOICED TO DATE $99,667	

United States Army Research Office (ARO) Small Business Technology Transfer (STTR) Program

Dr. Hongjun Zeng, Advanced Diamond Technologies, Inc.

Michael C. McAlpine, Assistant Professor, Department of Mechanical and Aerospace Engineering, Princeton University

Statement of Problem being Studied

In this STTR phase I project, Advanced Diamond Technologies worked with Princeton University to fabricate and characterize Strain-Modulated Diamond Nanostructures for Next-Generation, Biocompatible Nanoelectromechanical Systems.

Summary of the Most Important Results

- Delivered diamond film with designed thinness, grain size and doping levels for the fabrication of diamond nanoribbons.
- Developed stress control of diamond film to facilitate ribbons release.
- Studied pinhole density of diamond film and developed two new methods to decrease pinhole density for super thin (<100 nm) film.

- Fabricated diamond nanoribbons with diamond films of different doping levels and thicknesses. Notably, a 50-nm-thick film was demonstrated with good electrical continuity.

- Characterized diamond nanoribbons with SEM, EDS, AFM, Resistivity and gate effect measurement. Methods to improve the gate effect of diamond film were proposed.

- Florescence fibrinogen test protocol established. Accomplished mostly systematic fibrinogen test on different diamond surfaces. It showed ADT's UNCD more resistive to fibrinogen than MCD.

- EG6 diamond surface functionalization protocol optimized, demonstrating the capability of surface functionalization diamond nanoribbons for selective biosensing application.

Task Details

Task 1-1 Crystal size control- 100% done. Grain size was maximized (up to 100 nm) at 300 nm thickness. Grain size vs. doping level investigated. Smaller grain size also delivered for mechanical performance comparison.

In this task, we demonstrated two things: 1). Diamond as a rigid film with very high Young's Modulus, can be fabricated into flexible nanoribbons, which constitutes the technical platform for the whole project; 2). The diamond film can be reliably and uniformly doped, which allows continuation with sensor applications in Phase II. Our preliminary experiment showed that pin-holes appear when the diamond film thickness is ca. 1 μm and the film discontinuity increases as the thickness drops. At the same time, the thinner the film, the more flexible it is for ribbon formation; therefore we chose 300 nm as the regular thickness for minimum risk in the phase I project. We used the largest possible grain size while targeting the highest carrier mobility. Grain size control was performed by decreasing the CH_4/H_2 ratio (ca. 4 times) from ADT's regular Lighting25^{TM} recipe and increasing the chamber pressure (ca. 5 times). We also delivered ultrananocrystalline diamond (UNCD) films with smaller grain size and with two difference thicknesses (50 nm and 100 nm) to investigate their mechanical performance during nanoribbon fabrication. To investigate its semiconducting properties, diamond with 4 different levels of resistivity was deposited: 0.01-0.1 ohm·cm, 0.1-1 ohm·cm, 1-10 ohm·cm, and > 100 ohm·cm. The doping level was controlled by changing the TMB/CH_4 gas ratio. CH_4 and H_2 flow rates and the voltage applied on the filament were adjusted slightly to maintain the substrate temperature and diamond chemistry. The B/C (boron/carbon) ratio vs. the resistivity is listed in Table I, where the resistivity was measured by a four-point probe resistivity meter (Pro 4, Lucas Labs, with Keithley digital multimeter).

Table I Samples with various B/C ratios and resistivity levels. (* this ratio is an estimate)

Sample IDs	Recipe name	B/C ratio (ppm)	4PP film Resistivity (ohm·cm)	4pp ribbons Resistivity (ohm*cm)	Standard Error of Mean (ohm*cm)	Number of Devices
19457	A100HTP3	<10*	>100	∞	-	4
19309	ARO10ohm	120	8.56	14.2	*0.36*	4
19448	ARO1ohm	240	0.76	1.31	*0.079*	4
19959	ARO10mom	1200	0.066	0.09	*0.004*	5
8086	WF600B07	3000	0.02	0.01	*0.00034*	4
15743	WF600B05	3000	0.02	0.03	*0.0018*	4

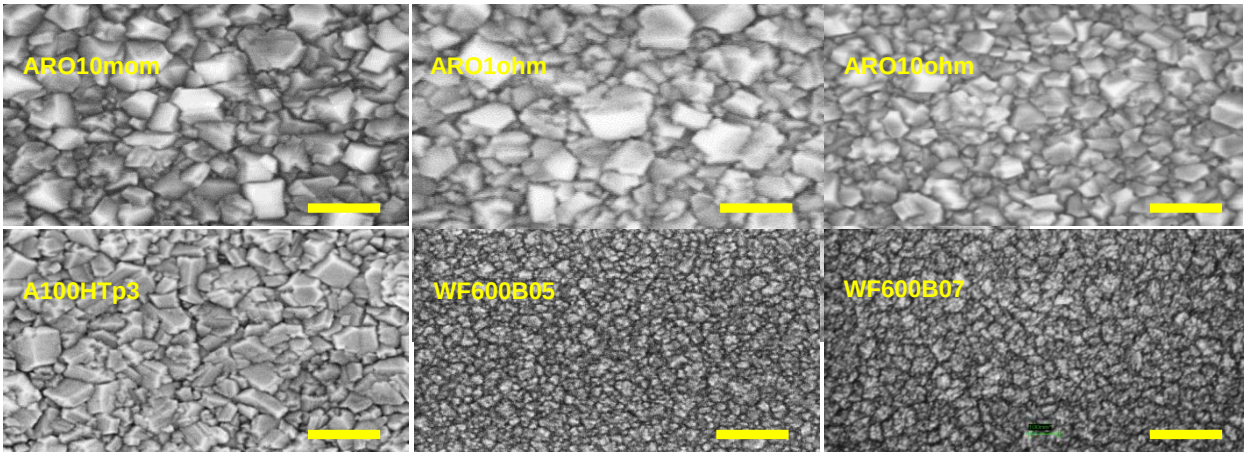

Fig.1 SEM images of diamond samples. Scale bars in figure represent 200 nm

SEM images in Fig.1 show that diamond films with all four levels of doping (listed in Table I) have almost the same grain size, in the range of 50-150 nm; however, the images also indicate that the dominant texture in diamond films with higher boron doping levels is likely (100), while in films with a lower doping level tends to form (111) texture. This result differs from a previous report[1] and will require further confirmation since the crystal size is still too small to exhibit an obvious orientation evolution. SEM images of UNCD show a much smaller grain size, about 3-5 nm. The grain clusters of 50-nm-thick films look slightly larger than those of 100- nm-thick films; this can be explained byte average seeding density: The gaps between the nucleation centers in the 50 nm film have not

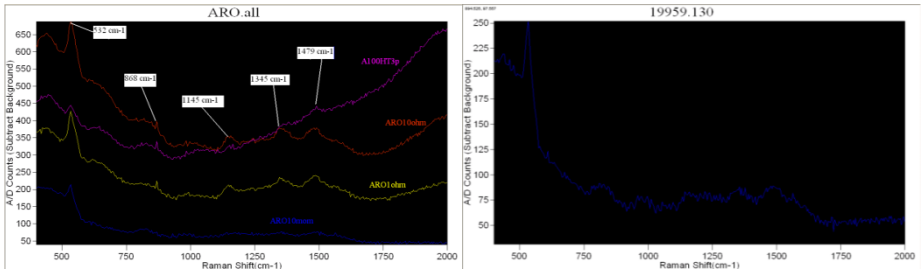

Fig. 2 Raman spectra (λ=532 nm) of (a) all diamond with different doping level and (b) diamond only with recipe “ARO10mom”

been fully filled, whereas in 100-nm thick films they are and re-nucleation proceeds more uniformly. This implies that 50 nm films are the thinnest we can achieve with acceptable film continuity.

The diamond signature can be identified in Raman spectra of the films produced, as presented in Fig. 2a. Spectra of recipe "ARO10ohm" and "ARO1ohm" exhibit typical nanocrystalline diamond (NCD) characteristics, with peaks at 1478 cm^{-1}, 1345 cm^{-1} and 1145 cm^{-1}, suggesting the existence of trans-polyacetylene, D-band graphite and nanocryalline diamond structure.[2] The spectrum of the recipe "A100HT3p" exhibits a different overall profile, but the spectrum still contains the principal peaks of NCD. Fig.2a also suggests that the Raman signals become weaker as the doping level increases, therefore the fine spectrum structures of the recipe "ARO10mom" cannot be easily seen. However, its separated spectrum presented in Fig.2b reveals similar main peaks.

Task 1-2: Engineering of mechanical properties of diamond film-100% done. Stress control developed. Film with proper compressive stress delivered to facilitate ribbons release.

A film with thickness of 300 nm usually has compressive stress of about -500 MPa. It was observed that a film at this stress level immediately cracks into very small pieces if it is released from the substrate. However, at very low stress, the film tends not to leave the substrate especially under capillary force when any liquid is present. Therefore, a relatively low stress, between 300-400 MPa compressive, is an appropriate target for ribbon fabrication. To reduce the residual stress of the film, a step is added in the recipe, by smoothly decreasing the CH_4/H_2 gas ratio, from ~5% to 0%, after the major deposition steps are completed. Since only the temperature increases during this short step, and there is not enough C for any deposition, the additional growth of the diamond is negligible, so the method is very suitable to control the stress in the thin film thickness regime. With this method, diamond films were produced at a temperature between 650-700 ˚C, ~50 ˚C lower than that for NCD production. A more comprehensive study on the relationship between stress, temperature, film thickness and ribbon performance will be conducted in Phase II.

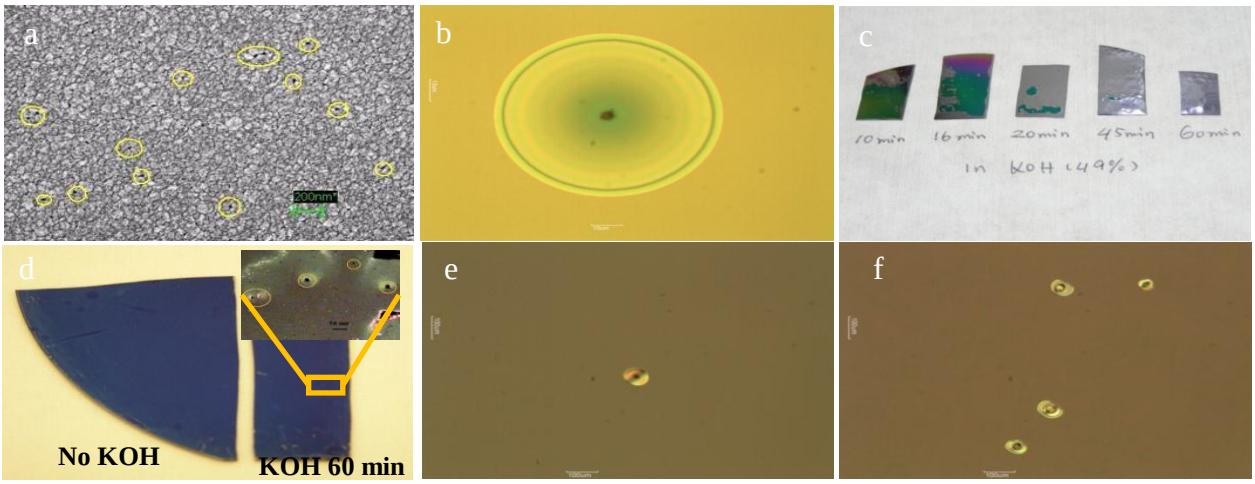

Fig. 3 (a) Real pin-holes under SEM in a 40 nm think diamond film and (b). Micrograph of SiO_2 defects caused by HF through a pin-hole in diamond film. KOH pin-hole test in (c) diamond films produced from regular UDD seeding process, (d) diamond film produced from PMMA-seeding method. Inserted image shows the pin-holes, highlighted by yellow circles, in this film after 60 minutes KOH test; HF pin-hole test in diamond film of (e) grow by double seeded method and (f) conventional single seeded method.

Task 1-3: Film continuity and pin-hole density. Pinhole density of as-deposited films were studied. Two new methods for fabricating super thin (<100 nm) film with lower pin-hole density were demonstrated.

According to the experimental results, when the diamond is thinner than 50 nm, pin-holes can be directly observed in a SEM (Fig.3a). When the thickness increases, pin-holes are hidden in the film and become difficult or impossible to observe and count under SEM inspection. Therefore a HF or KOH test protocol was introduced to detect and count pin-holes in diamond on SiO_2 or Si substrates. If there is a pinhole, the HF or KOH etchants can quickly penetrate the film, etch the underlying substrate and thereby leave a readily observable "etch mark" in the SiO_2 or Si wafer, respectively. Fig.3b shows a typical pinhole-caused circular etching boundary in a SiO_2 layer after a HF test. With this protocol, it was observed that pinhole density in a film thicker than 1.5-μm is 0, i.e. the film is "pinhole free", but that the pinhole density increases as the thickness is decreased. A 300-nm-thick film has a pinhole density of 100-700/cm^2.

Two preliminary techniques to decrease pinhole density were developed. In the first, diamond seeds with average size of 5-8 nm (Opal seeds from International Technology Center) mixed with liquid Poly(methyl methacrylate) (PMMA- MicroChem PMMA495C5). This PMMA was then thinned with chlorobenzene in order to achieve a <50-nm-thick PMMA film after drying. The PMMA-seed solution was then spin coated on a Si wafer followed by a soft bake at 100 ˚C. The seeded wafer was coated with about 100 nm diamond and went through a KOH pin-hole test. Fig.3c is the test on a 250 nm thick diamond film produced with a regular seeding process. About 300 pinholes/cm^2 were counted in the film after a 16-minute test, and the film was completely etched away in 60 minutes. In contrast, the film spin-seeded with PMMA-seed solution survived a 60-minute test. A ~50 /cm^2 pinhole density was evaluated for this film. In this preliminary experiment, the pinhole distribution was not uniform. The insert image in the Fig. 3 (right) is the micrograph of the area exhibiting the densest pinholes. Nevertheless, it shows that the new seeding method delivers a lower pinhole density. In the second process, SiO_2 wafers were seeded with a conventional seeding technique, and then loaded into the reactor for a

deposition run of only 2-6 minutes, followed by a second seeding and coating with 500 nm diamond. The wafers were tested under the HF pinhole counting protocol, and compared with a control sample of regular, single seeded film with the same thickness. As shown in Fig. 3e, The pinhole density in the control film was 27/cm^2, while the re-seeded films' pinhole density was only 2-7/cm^2 (Fig.3f) demonstrating ~ 5X lower pin-hole density than the former control sample.

Task 2: Engineering of electronic and mechanical properties

Task 2-1: Diamond strain engineering with nanostructure buckling- 100% done. Diamond nanoribbons were fabricated with diamond films of different doping levels and thicknesses. Notably, a 50- nm-thick film was successfully converted into nanoribbons, demonstrating acceptable film continuity.

We have previously shown that flat or buckled piezoelectric nanoribbons of PZT can be generated over large areas on PDMS substrates via a parallel printing process.[3-4] Similarly, in this project nanopatterned diamond structures were transferred to PDMS by etching the underlying sacrificial SiO_2/Si to free the nanocrystalline diamond structures from the host wafer and form nanoribbons. Further, ensuring the diamond ribbons have nanometer scale dimensions is critical for the ultimate performance of these materials. Indeed, as the maximum deflection of a ribbon is: $x = SL^2/t$, where S is the maximum surface strain (S~ 10^{-3}), L is the ribbon length (L~ 1 mm) and t is the thickness, cm-scale deflections can only be achieved for sub-100 nm diamond film thicknesses. This approach also lends itself to ease of nanofabrication, since the growth process – in this case, CVD of diamond nanofilms – can be used to control the nanometer-scale thickness dimension, while photolithography and etching can be used to define the nanoribbon widths and lengths. Indeed, both 100 nm and 50 nm thick diamond films were successfully fabricated into ribbons, which encourage us to use such (or even thinner) films for the sensor fabrication in Phase II.

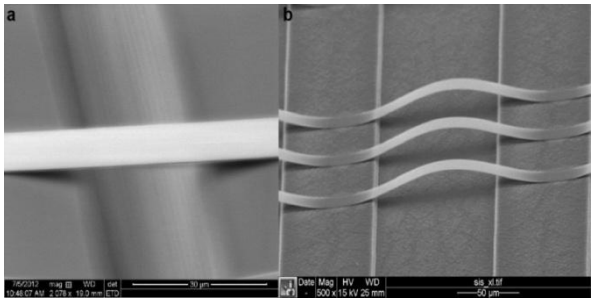

Fig. 4 SEM images of (left) flat diamond ribbon suspended across a 20 μm wide and 30 μm deep trench and (right) buckled diamond ribbons on elastomeric PDMS substrate.

Our printing process consisted of the following steps: 1) diamond nanofilms were deposited and patterned into nanoribbons by lithography and etching, 2) etching of the underlying SiO_2 using HF to free the diamond nanoribbons from their host. The exposed SiO_2 between the diamond nanoribbons provides an avenue for the acid to undercut and loosen the ribbons without dislocating them; 3) Transfer printing of diamond ribbons. A slab of PDMS (~2 mm thick) was brought into conformal contact with the ribbons. For the generation of buckled structures, the PDMS was elastically pre-stretched before contact. Peeling off the PDMS allowed the transfer of the diamond ribbons to the elastomer via adhesive van der Waals forces. Fig. 4a shows an SEM image of the ribbons transferred using unstrained PDMS, while Fig.4b shows the ribbons with a wavy/buckle structure induced by relaxing prestrained PDMS.

Task 2-2: Strain-Enhanced Properties. -100% done. Diamond Nanoribbons geometry and performance were characterized by SEM, EDS, AFM. Resistivity, gate effect and flexoelectricity of ribbons were studied. Methods to improve the gate effect and flexoelectrical performance were proposed. Diamond Nanoribbon processing with high flexibility and reliability for advanced nanoelectromechancial systems based on strain-modulated diamond has been established.

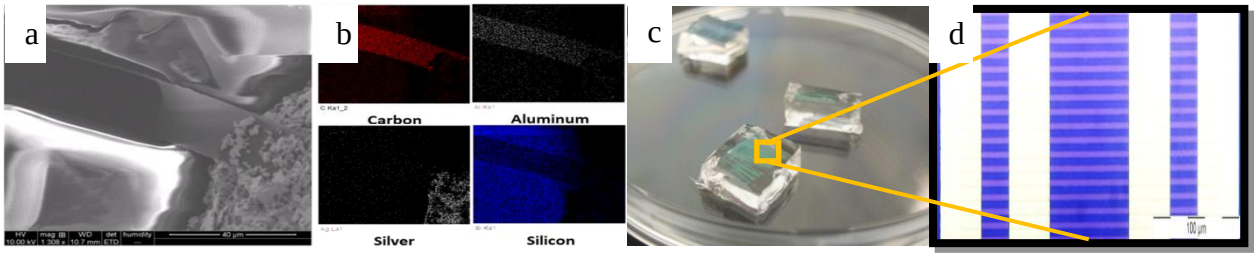

Fig. 5 (a) Elemental composition maps of diamond nanoribbon with associated electrodes and (b) underlying Si substrate imaged by EDX, (c) nanoribbon array transferred on PDMS stab and (d) the magnified details of the nanoribbon array

Fig.5a-b show the elemental composition of the diamond nanobuckled system, which also includes side electrodes (Ag paint) and an electrode along the buckle length (Al), along with the underlying Si substrate. Fig. 5c-d show PDMS slabs containing diamond nanoribbon arrays. The smallest ribbon is 50 nm thick, 3 μm in width and 25 μm in length. Each array was connected with 4 electrodes (10 nm Ti, 100 nm Au), which enabled four terminal sensing to minimize the effect of contact resistance. Each device contains 200 nanoribbons to improve analyte transport, which should increase the overall detection sensitivity. The electrodes were insulated with 500 nm of Silicon Nitride and a PDMS channel was attached to the diamond array for real time solution measurement.

Diamond nanoribbons with six different doping levels have been completed as described in task 2-1. Four to five devices were fabricated for each condition. From I-V measurement, the electrical contact was asserted to be ohmic. For the purpose of solution gate measurements, a layer of 1.5-μm-thick SU-8 2002 photoresist was defined with photolithography at the last stage of fabrication. The SU-8 forms an insulating layer that completely covers the electrodes to prevent leakage currents and thus, minimizes electrical noise. Table I shows the results of 4-point probe measurements of the devices' resistivity; the resistivities encountered are of the same order of magnitude with the resistivity of the films measured before release. Such an agreement suggests that even with 50 nm thickness, the films are electrically continuous. The experiment also demonstrates the robustness of the diamond film, which enables consistent and reproducible device fabrication, in contrast to other nano-materials such as graphene. This means a solid diamond nanoribbons technology is ready for developing and characterization of biosensors based on strain-modulated diamond nanostructures.

Table II Transconductance of diamond related with dopant at 300K

Dopant	Transconductance (mS/mm)
B	1.0×10^{-4}
Al	1.2×10^{2}
Be	1.5×10^{2}
Ca	1.1×10^{2}
Cd	9.0×10
Ga	8.0×10
In	1.0×10^{2}
Li	1.1×10^{2}
Mg	1.2×10^{2}
Zn	9.0×10

The gating characteristics of the devices have been carefully investigated. Indium was applied on the silicon substrate at the back of the wafer. The device source- drain voltage is biased at -0.1V and a gate voltage from 0 to -5V was applied Six devices investigated did not show significant gating effect. Results are similar for solution gate measurement with Ag/AgCl electrodes with a gate voltage from 0 to -0.5V (larger gate voltage causes dielectric break down, as the diamond nanoribbons surface is not fully hydrogen terminated), so far we have not observed the diamond nanoribbons have strong gating effects among all doping levels we delivered in phase I. the transconductance of the diamond nanostructure was barely detectable. Literature[5] shows that boron-doped diamond does not exhibit strong gating effect as compared to other dopant types. Table II shows transconductances of single crystal diamond film transistor devices corresponding to doping with different elements. The low tranconductance of boron-doped diamond transistors is due to the very low hole concentration, which is only of the order of 10^{14} cm^{-3} at room temperature, even when the B-atom concentration is as high as $1.0\times10^{21}cm^{-3}$. Hence, a different dopant strategy could potentially be used to significantly enhance the transconductance of the diamond film, including alternative thermal treatments. Hydrogen-induced surface conductive channels showed more promising results than other doping strategies for the fabrication of diamond MESFET (metal semiconductor field effect transistor).[6-7] We plan to introduce such a surface channel technique with hydrogen termination on diamond surface, and combine it to the diamond nanostructure fabrication technique to achieve high sensitivity. This issue will be intensively addressed in the phase II project.

Table III diamond with different surface chemistry for fibrinogen absorption test

sample #	Description		
	Surface Termination	Dopant	Polished?
A	UNCD as-dep	No	No
B	UNCD as-dep, H_2	No	No
C	UNCD as-dep	Yes	No
D	UNCD as-dep, H_2	Yes	No
E	UNCD as-dep	Yes	Yes
F	UNCD as-dep, H_2	Yes	Yes
G	UNCD as-dep	No	Yes
H	UNCD as-dep, H_2	No	Yes
I	UNCD SiO_2	control	
J	UNCD SiO_2, H_2	control	
K	MCD as-dep		
L	MCD as-dep, H_2		

Task 3: Surface Chemistry of nanoribbons

Task 3-1: Biocompatibility study. -100% done- Florescence fibrinogen test protocol established. Accomplished mostly systematic fibrinogen test on different diamond surfaces. It shows UNCD and doped UNCD both more resistive to thrombosis than MCD.

In this phase I project, we studied the biocompatibility of the diamond ribbon surface by observing fibrinogen absorption on the surface. Since the degree of surface adhesion to fibrinogen is a measure of the interactivity of diamond surface with the human blood clotting mechanism, adhesion to fibrinogen can be used as an indication of the surface bioinertness. The fibrinogen test protocol is consisted of the following: Two samples for each of the surfaces listed in Table II were prepared by sonication and/or rinsing in ethanol and dried with a stream of N_2.

One of these samples for each surface was set aside as reference for the fluorescence measurements. On each type of sample surface three spots were placed, consisting of a solution of ~0.2-0.4 mg/ml fluorescence tagged fibrinogen (Alexa Fluor 546 conjugate) in 0.1M NaHCO3 for 1 hr at 37 ˚C. Rinsing followed, including an initial 15 min. soak in 2X SSPE (Saline Sodium Phosphate EDTA) w/1% Triton x-100, a 5 min. soak in 2X SSPE, and two 5 min. soaking in deionized water. To avoid evaporation, the samples were kept in a hybridization chamber hydrated with droplets of PBS (Phosphate buffered saline). An optical microscope with Hg lamp was used to capture the fluorescent image of the spots and on a background region surrounding the spot with 4s exposure. Basically the darker the field of view, the less fibrinogen is absorbed on the surface.

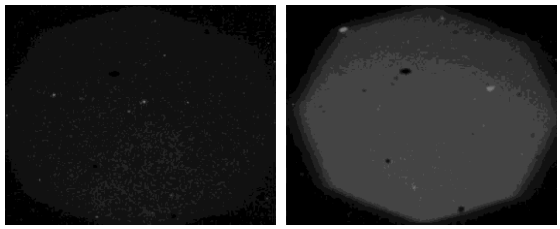

Fig.6 Fibrinogen adsorption studies on two types of UNCD surfaces: (left) as-deposited UNCD and (right) UV-oxidized UNCD, control. The droplets are 50 microL. The fibrinogen concentration is 0.2 mg/mL. The stock solution is 1.5 mg/mL after adding 3.33 mL to lypolized powder

We first completed the initial validation tests of the fibrinogen adsorption protocol on two types of the original diamond surfaces, as-deposited and oxidized (excited by UV light at 254 nm for 60 min), as shown in Fig. 6. The oxidized sample was chosen to have a preliminary evaluation of the effect of O/C ratio on fibrinogen adsorption. We expected the surface of diamond nanoribbons to have their O/C ratio altered during processing. From these data, the as-deposited diamond with low O/C ratio shows reduced fibrinogen adsorption, as expected. We then prepared 12 types of diamond film for the biocompatibility test using the same fibrinogen

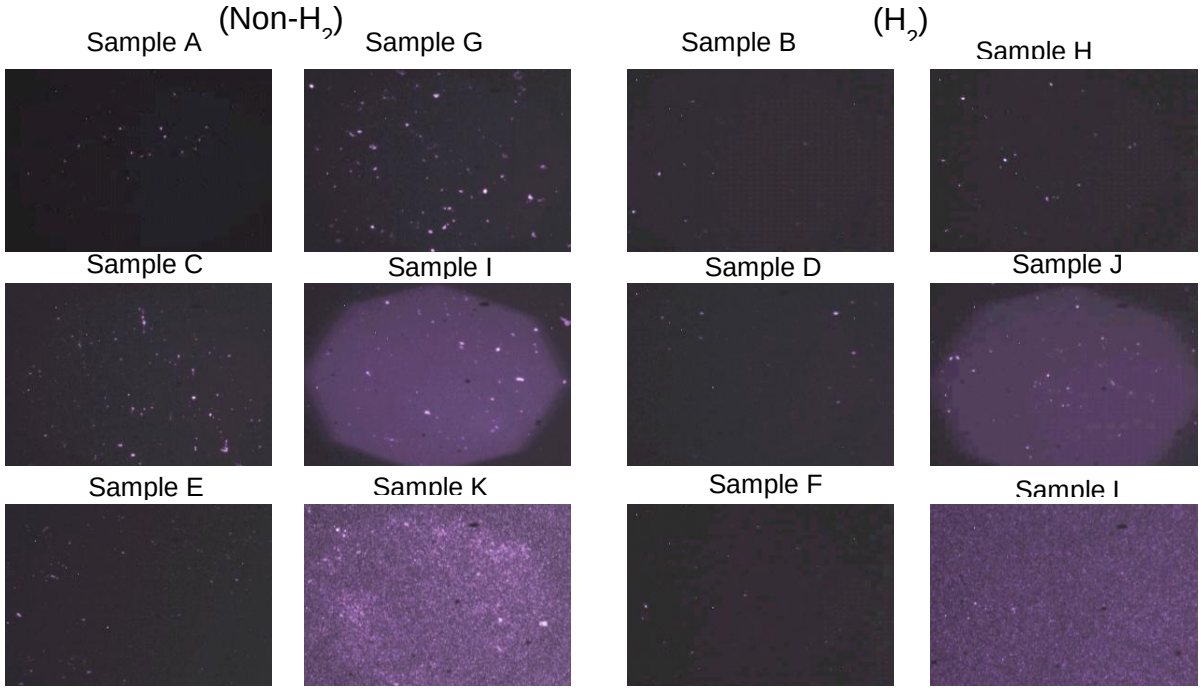

Fig. 7 Florescence images of diamond with different surface chemistry. Sample I and J are control, SiO2 and SiO2 with Hydrogen treatment.

absorption protocol validated above. Table III is the list of these films. The main observations of the testing, as shown in Fig.7, are: 1) fibrinogen adsorption was found to be slightly higher for boron-doped diamond. (2) Similar levels of adsorption were noted for doped, un-polished and un-doped, polished surfaces. Less adsorption was noted for a doped, polished surface when compared to the other two surfaces. (3) Interestingly, the microcrystalline diamond (MCD, sample K and L), showed a higher fibrinogen adsorption. This might be due to its rougher surface, which is similar to higher adsorptions noted on rougher MCD surfaces. Smooth UNCD showed significantly stronger fibrinogen resistance. In the future, if MCD is needed for some purpose such as high carrier mobility, we can adjust the deposition chemistry at the end of the whole deposition such that the major thickness is still MCD, while a thin UNCD layer is formed on top. That way, the full biocompatibility of the film can be ensured as well. (4) Fibrinogen adsorption was most significant on the control silicon dioxide surface. The results suggest that in order to reduce fibrinogen adsorption, un-doped surfaces are better. If the application requires a doped surface, then a smoother, polished surface is better. 5). All hydrogen-treated surfaces are better than all the un-treated surfaces.

Task 3-2: Surface functionalization. 100% done-EG6 diamond surface functionalization protocol optimized.

We practiced the diamond surface functionalization with the following optimized protocol: 1) Sonicate two chips of the same surface termination (as-deposited, oxidized or H_2 terminated) (~15 mm squares) and quartz cover slip in ethanol for 5 min. Rinse and dry with a stream of N_2. Keep one chip aside for background measurement. Thaw EG6 in dark. 2) Put 1-2 drops of EG6 on chip and place the cover slip on it. Assemble in UV box. Flow a stream of N_2 through the chamber for 15 min. 3) Expose to UV light at 254 nm for 12 h. 4) Rinse chip and cover slip with EtOH. Dry with N_2. 4). Incubate with ~0.2 mg/ml fibrinogen (Alexa Fluor 546 conjugate) in 0.1 M $NaHCO_3$ for 1 h at 37°C in a hybridization chamber, and 5) Soak in 2X SSPE w/1% Triton X-100 (15 min), then soak in 2X SSPE (5 min) and soak in DI H_2O (2X, 5min).

The molecule EG6 (Molecular Probes) was grafted to the surfaces to investigate the influence of ethylene glycol oligomers on reducing the nonspecific binding of fibrinogen. EG6 binds to diamond surfaces via the olefin group when excited by UV light at 254 nm. A fluorescence imager was used to evaluate the fluorescence intensity within each spot, and on a background region surrounding the spot that was not exposed to fibrinogen. For dynamic, reliability tests under flow conditions, a custom flow cell was designed and micro fabricated. A solution containing ~0.15 mg/ml fluorescence-tagged fibrinogen (Alexa Fluor 546 conjugate) in 0.1 M $NaHCO_3$ was flown (~100 µL/min) in recycle mode from a container maintained at 37 ^oC in a heat block. The experiment showed that the overall reduction in non-specific fibrinogen adsorption for both hydrogen-terminated and hydrogen-terminated-EG6 UNCD is a positive result for implantable devices coated with UNCD films since it is easier to terminate a surface with hydrogen than it is to coat EG6 monolayers on a complex 3D surface. This result validates the preliminary surface functionalization, which will be further developed to improve selectivity of biosensors based on the strain-modulated diamond nanostructures.

References

Locher, R., Wagner, J., Fuchs, F., Maier, M., Gonon, P., Koidl, P., Optical and electrical characterization of boron-doped diamond films, Diamond and Related Materials 4 (1995)

Qiang Hu, Makoto Hirai, Rakesh K Joshi and Ashok Kumar, Structural and electrical characteristics nitrogen-doped nanocrystalline films prepared by CVD, J. Phys. D: Appl. Phys. 42 (2009) 025301 (4pp)

Qi, Y. et al. Piezoelectric ribbons printed onto rubber for flexible energy conversion. Nano Lett. 10, 524-528 (2010).

Feng, X, et al., Stretchable Ferroelectric Nanoribbons with Wavy Configurations on Elastomeric Substrates, ACS Nano, 5, 3326–3332(2011)

EP Patent 2,400,533, 2011

C. E. Nebel, et al., Surface electronic properties of H-terminated diamond in contact with adsorbates and electrolytes, phys. stat. sol. (a) 203, No. 13, 3273–3298 (2006)

Y. Gurbuz, et al, Diamond semiconductor technology for RF device applications, Solid-State Electronics 49 (2005) 1055–1070